Simulation of viscoelastic two-phase flows with LS-DYNA ICFD

Z. Solomenko[1], F. Del Pin[1], I. Caldichoury[1]

[1]Ansys

1 Introduction

Simulations of viscoelastic flows are presented. Viscoelasticity is accounted for by solving a constitutive equation for the conformation tensor - the viscoelastic stress tensor is directly related to the conformation tensor [1] and the divergence of the viscoelastic stress tensor yields an extra momentum source. The Oldroyd-B constitutive model is here considered [1]. Results of several benchmark tests are presented. Implementation is first tested on a two-dimensional lid-driven cavity flow. Results of two-dimensional and three-dimensional Oldroyd-B liquid jets are then presented. Viscoelastic models are used in applications like food-processing, polymer melt processing, blood flow modeling.

2 Theory

The constitutive model equation needs to be solved for the conformation tensor. Let μ_p and λ be the polymeric viscosity and the relaxation time, respectively. The constitutive equation reads

$$\frac{\partial A}{\partial t} + \boldsymbol{u} \cdot \nabla A - \nabla \boldsymbol{u} \cdot A - A \cdot \nabla \boldsymbol{u}^T = -\frac{1}{\lambda} f_R(A),$$

with f_R a relaxation function. The constitutive equation is solved in the log-conformation framework, for the code to be able to handle flows with high viscoelasticity, *i.e*. high-Weissenberg number [2]. The viscoelastic tensor reads

$$\tau = \frac{\mu_p}{\lambda} f_S(A),$$

with f_S a strain function. The divergence of the viscoelastic tensor is an extra term in the momentum equation. For an Oldroyd-B fluid, relaxation and strain functions are such that $f_R(A) = f_S(A) = A - I$.

3 Features

`*ICFD_MODEL_VISCOELASTIC`

This specifies parameters of the viscoelastic model, which must be referenced in the material card.

`*ICFD_BOUNDARY_PRESCRIBED_VISCOELASTIC`

This specifies boundary conditions for the conformation tensor. In practice, boundary conditions for the conformation tensor are not mandatory, but it is better to specify them when the velocity is prescribed.

Note that a relaxed state $A = I$ is considered as initial condition.

4 Some results

4.1 Two-dimensional lid-driven cavity flow

This is the standard benchmark test that was studied in detail in [2]. Consider a square cavity of side L. The top boundary has an imposed profile

$$\boldsymbol{u}(\boldsymbol{x}, t) = 8U(1 + \tanh(8t - 4))x^2(1 - x)^2 \boldsymbol{e}_x,$$

with x and t made dimensionless by using L and L/U as characteristic length and time. No-slip is imposed at remaining boundaries. The fraction of solvent viscosity is $\beta = 0.5$. The Reynolds number is $Re = 0.01$. The Weissenberg number is $Wi = 1$. The timestep is $\Delta t = 5 \cdot 10^{-5}$. Simulations were run on three meshes, details of which are given in Tab.1. Results of velocity profiles are shown in Fig.1. Results compare very well with previous work [2]. Convergence of velocity profiles to M3 results is linear.

Mesh	M1	M2	M3
minh	1/80	1/160	1/320
maxh	1/40	1/40	1/80

Table 1: Mesh details for the two-dimensional lid-driven cavity flow.

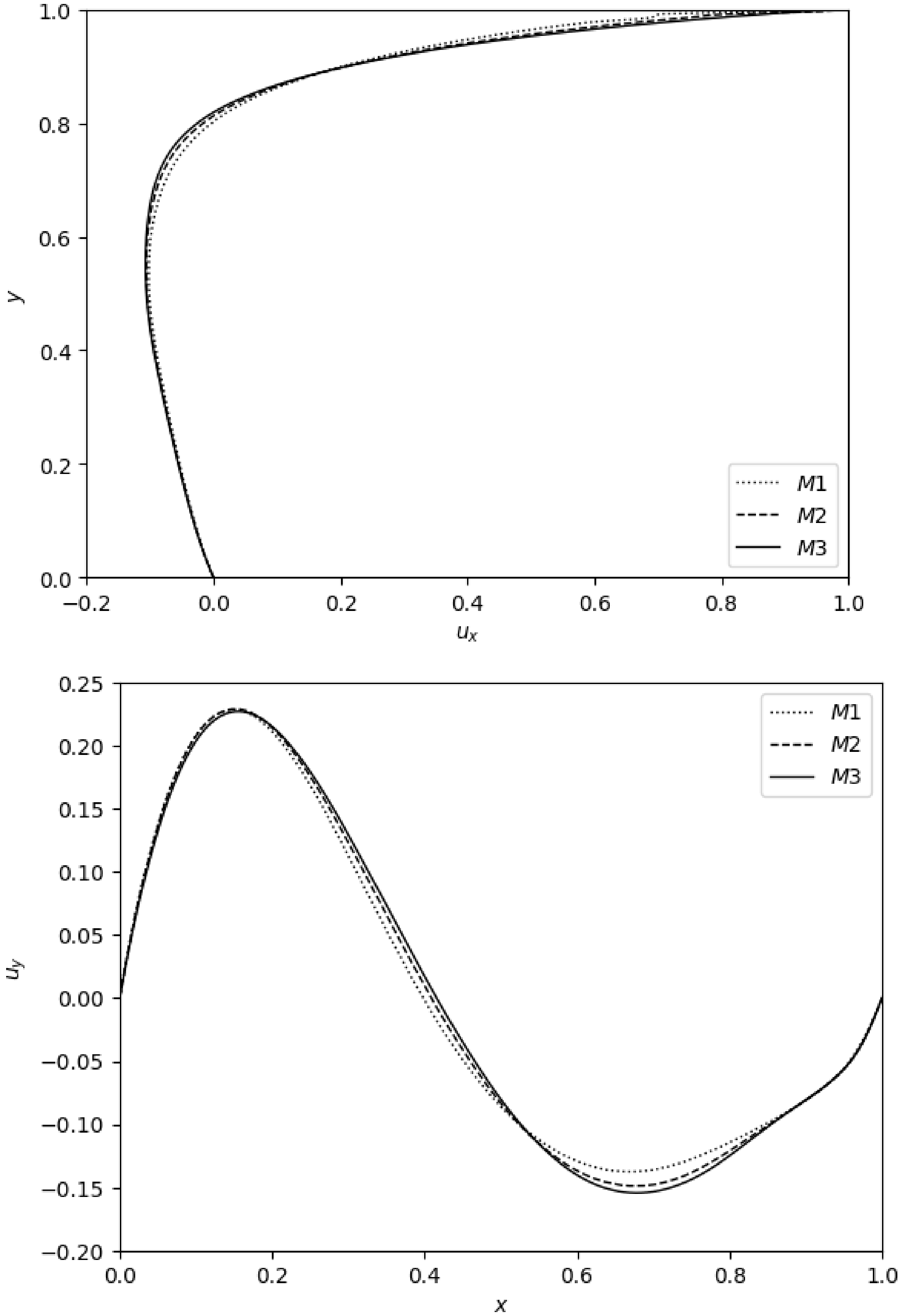

Fig.1: Velocity profiles $u_x(0.5, y)$ and $u_y(x, 0.5)$ at $t = 8$ for the two-dimensional lid-driven cavity flow.

4.2 Two-dimensional jet buckling

That is a benchmark for two-phase viscoelastic flow without surface tension [3]. A liquid jet flows down into the air. Simulations of Newtonian and viscoelastic flows are compared.

4.2.1 Newtonian fluid

Inlet is positioned at $(0, H)$ and has a width L. Fluid is injected down with a velocity $(0, -U)$. Parameters are gathered in Tab.2 – those correspond to Reynolds and Froude numbers $Re = 0.01$ and $Fr = 0.5$.

H	L	U	P	μ_s	g
0.075 m	0.004 m	0.1 $m.s^{-1}$	1000 $kg.m^{-3}$	40 Pa.s	9.81 $m.s^{-2}$

Table 2: Simulation parameters for Newtonian liquid jet.

4.2.2 Oldroyd-B fluid

Same flow parameters are used here except for the solvent viscosity. New parameters are gathered in Tab.3 – those correspond to a fraction of solvent viscosity $\beta = 0.1$ and a Weissenberg number $Wi = 20$.

μ_s	μ_p	Λ
4 Pa.s	36 Pa.s	0.8 s

Table 3: Simulation parameters for Oldroyd-B liquid jet.

4.2.3 Results

Time-stepping was based on a maximum CFL of 0.5. Qualitative results are given in Fig.2 – viscoelasticity yields less viscous dissipation, and more stretching compared to the Newtonian flow. Three meshes were used for convergence tests – see details in Tab.4. Time signals of the normalized jet length are shown in Fig. 3. Results compare very well with those from the literature [3,4].

Mesh	M1	M2	M3
minh	1/20	1/40	1/80

Table 4: Mesh details for two-dimensional liquid jets.

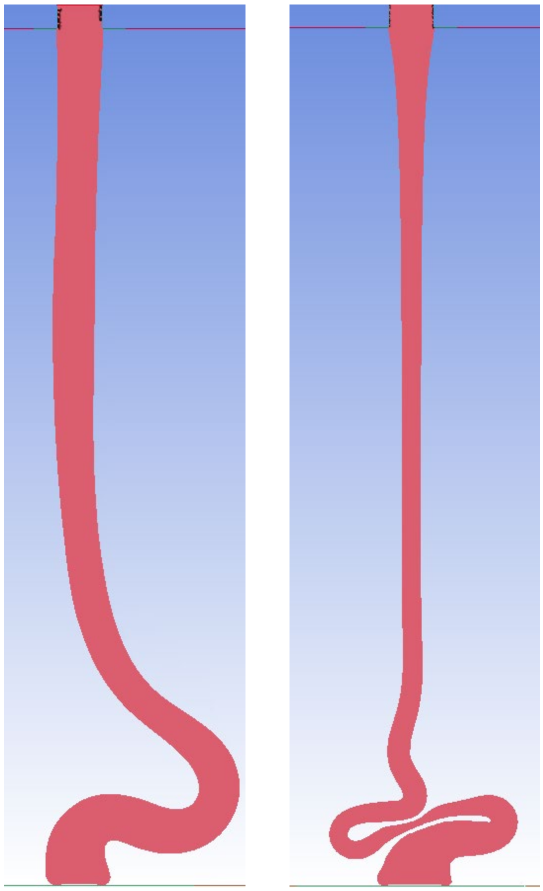

Fig.2: Left: Newtonian jet at $t = 20$*. Right: Oldroyd-B jet at* $t = 13.25$*.*

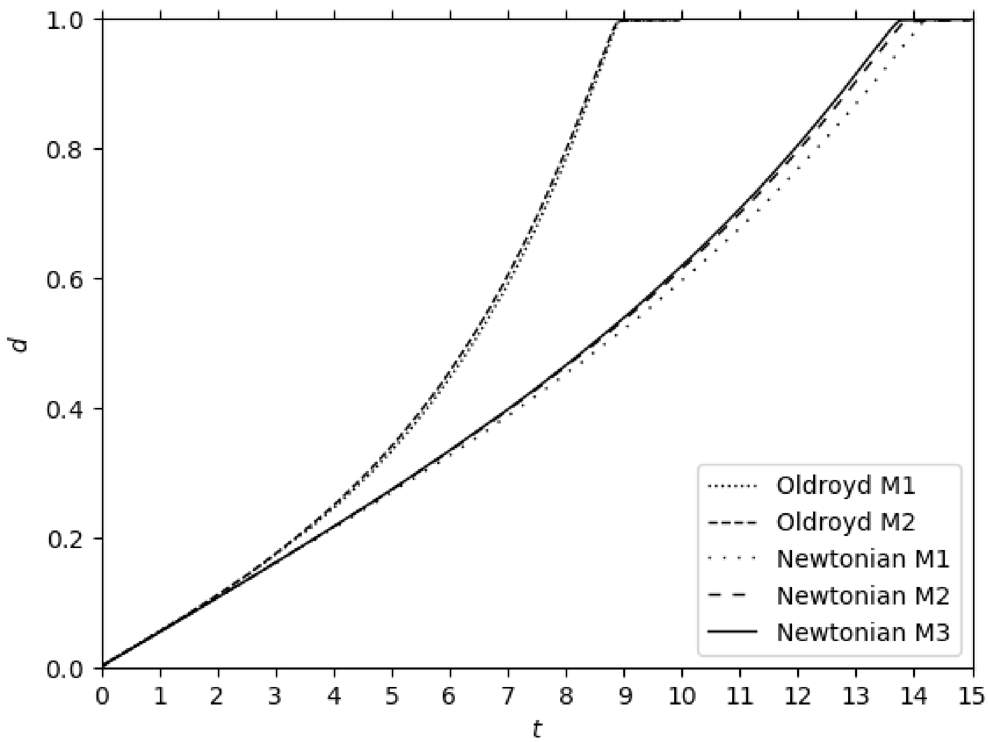

Fig.3: Time signals of jet length. Time and jet length are made dimensionless with L/U *and H, respectively.*

4.3 Three-dimensional jet buckling

The case from Section 4.2 is now extended to three dimensions, as in [4]. Fig.4 shows qualitative results for the Oldroyd-B jet, obtained with a uniform mesh size 1/20. As in [4], the jet reaches the bottom wall earlier than in the two-dimensional case. Results compare well with those from [4].

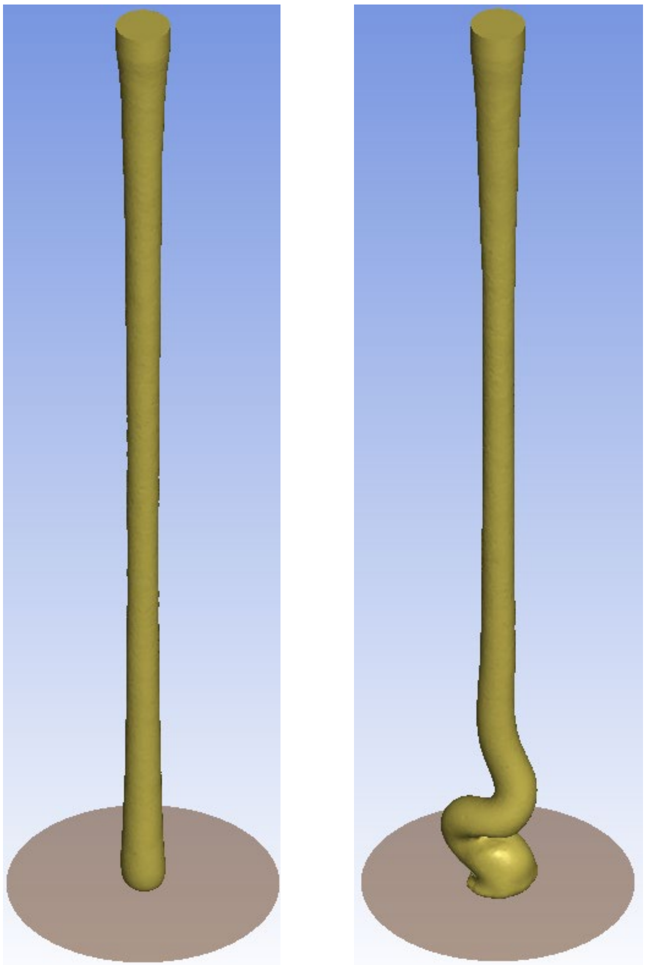

Fig.4: Oldroyd-B jet at times $t = 8.25$ *and* $t = 10.25$.

5 Summary

Oldroyd-B single and two-phase flows can now be simulated with ICFD. Future work will focus on extension to other constitutive models by using different relaxation and strain functions. The code will also be tested on more complex models, *e.g.* viscoelastic flows with surface tension.

6 Literature

[1] Alves, M. A., Oliveira, P. J., & Pinho, F. T. (2021). Numerical methods for viscoelastic fluid flows. *Annual Review of Fluid Mechanics*, *53*, 509-541.
[2] Fattal, R., & Kupferman, R. (2005). Time-dependent simulation of viscoelastic flows at high Weissenberg number using the log-conformation representation. *Journal of Non-Newtonian Fluid Mechanics*, *126*(1), 23-37.
[3] Oishi, C. M., Martins, F. P., Tomé, M. F., & Alves, M. A. (2012). Numerical simulation of drop impact and jet buckling problems using the eXtended Pom–Pom model. *Journal of Non-Newtonian Fluid Mechanics*, *169*, 91-103.
[4] Rizzieri, G., Ferrara, L., & Cremonesi, M. (2024). Simulation of viscoelastic free-surface flows with the Particle Finite Element Method. *Computational Particle Mechanics*, 1-25.